THE JOURNAL OF BIOLOGICAL CHEMISTRY
Vol. 278, No. 46, Issue of November 14, pp. 45858–45863, 2003
Printed in U.S.A.

The Structural Determination of Phosphosulfolactate Synthase from *Methanococcus jannaschii* at 1.7-Å Resolution

AN ENOLASE THAT IS NOT AN ENOLASE*

Received for publication, July 11, 2003, and in revised form, August 26, 2003
Published, JBC Papers in Press, September 2, 2003, DOI 10.1074/jbc.M307486200

Eric L. Wise‡§, David E. Graham¶‖, Robert H. White¶, and Ivan Rayment‡**

From the ‡Department of Biochemistry, University of Wisconsin, Madison, Wisconsin 53706 and the ¶Department of Biochemistry, Virginia Polytechnic Institute and State University, Blacksburg, Virginia 24061

Members of the enolase mechanistically diverse superfamily catalyze a wide variety of chemical reactions that are related by a common mechanistic feature, the abstraction of a proton adjacent to a carboxylate group. Recent investigations into the function and mechanism of the phosphosulfolactate synthase encoded by the *ComA* gene in *Methanococcus jannaschii* have suggested that ComA, which catalyzes the stereospecific Michael addition of sulfite to phosphoenolpyruvate to form phosphosulfolactate, may be a member of the enolase superfamily. The ComA-catalyzed reaction, the first step in the coenzyme M biosynthetic pathway, likely proceeds via a Mg^{2+} ion-stabilized enolate intermediate in a manner similar to that observed for members of the enolase superfamily. ComA, however, has no significant sequence similarity to any known enolase. Here we report the x-ray crystal structure of ComA to 1.7-Å resolution. The overall fold for ComA is an $(\alpha/\beta)_8$ barrel that assembles with two other ComA molecules to form a trimer in which three active sites are created at the subunit interfaces. From the positions of two ordered sulfate ions in the active site, a model for the binding of phosphoenolpyruvate and sulfite is proposed. Despite its mechanistic similarity to the enolase superfamily, the overall structure and active site architecture of ComA are unlike any member of the enolase superfamily, which suggests that ComA is not a member of the enolase superfamily but instead acquired an enolase-type mechanism through convergent evolution.

Mechanistically diverse superfamilies consist of groups of homologous enzymes that catalyze a wide variety of reactions related by a common mechanistic feature (1). When a new protein sequence can be ascribed to a superfamily, the function and mechanism of the enzyme can often be predicted, even for novel enzyme reactions (2). There are several well studied mechanistically diverse enzyme superfamilies, some of which may possess hundreds of members, each related to one another by a common mechanistic thread (1, 3). Understanding the breadth of these superfamilies will be essential to interpret the vast number of sequences identified by high throughput genome sequencing projects.

The enolase superfamily is a particularly well studied mechanistically diverse superfamily whose members catalyze diverse reactions that involve the abstraction of a weakly acidic proton (4). Each enzyme in this superfamily catalyzes a reaction that proceeds via an enolate intermediate that is derived from the abstraction of an α-proton from a carboxylate substrate that is stabilized by one or more Mg^{2+} ions in the active site.

The x-ray crystal structures of several enolase superfamily members have been solved. In all cases identified to date, these enzymes are constructed of a central $(\alpha/\beta)_8$ barrel domain and an $\alpha+\beta$ domain that is usually built from sequence at both the N and C termini (5–8). The $(\alpha/\beta)_8$ barrel domain contains the residues that act as ligands for the metal ion as well as those involved in acid/base catalysis. The $\alpha+\beta$ domain "caps" the active site at the C-terminal end of the barrel domain and has been proposed to confer substrate specificity on the individual members of the enolase superfamily (9). A comparison of the active sites of enolase superfamily members has shown that a triad of conserved aspartate and glutamate residues usually coordinates an essential metal ion found in the active site (4).

Members of the enolase superfamily have been assigned to one of three subgroups named after their enzyme prototypes: mandelate racemase, muconate lactonizing enzyme, and enolase (10). A key feature that delineates members of each subgroup is the identity of the residues that serve as the general base(s) for proton abstraction. In the case of the mandelate racemase subgroup, either a conserved lysine residue or a conserved histidine residue carries out this function. In the muconate lactonizing enzyme subgroup, two conserved lysine residues function as the general base(s), and in the enolase subgroup, one conserved lysine performs this function. Membership in one of these subgroups can be used to help infer enzyme function and mechanism, in some cases before biochemical evidence exists. For example, on the basis of sequence similarity to known members of the muconate lactonizing enzyme subgroup, two novel *Bacillus subtilis* enzymes were identified as L-Ala-D/L-Glu epimerases that catalyzed 1,1-proton transfer reactions (2).

Since many members of the enolase superfamily share less

* This work was supported by Grants GM-52594 (to I. R.) and GM-65155 (to I. R.) from the National Institutes of Health, National Science Foundation Grant MCB 0231319 (to R. H. W.), and a National Science Foundation grant (awarded to D. E. G. in 2002). Use of the Argonne National Laboratory Structural Biology Center beamline at the Advanced Photon Source was supported by the United States Department of Energy, Office of Energy Research, under Contract No. W-31-109-ENG-38. The costs of publication of this article were defrayed in part by the payment of page charges. This article must therefore be hereby marked "*advertisement*" in accordance with 18 U.S.C. Section 1734 solely to indicate this fact.

The atomic coordinates and structure factors (code 1QWG) have been deposited in the Protein Data Bank, Research Collaboratory for Structural Bioinformatics, Rutgers University, New Brunswick, NJ (http://www.rcsb.org/).

§ Supported by the National Institutes of Health Biophysics Training Grant GM08293.

‖ Present address: Dept. of Chemistry and Biochemistry, University of Texas at Austin, Austin, TX 78712.

** To whom correspondence should be addressed: Dept. of Biochemistry, 433 Babcock Dr., Madison, WI 53706. Tel.: 608-262-0437; Fax: 608-262-1319; E-mail: Ivan_Rayment@biochem.wisc.edu.

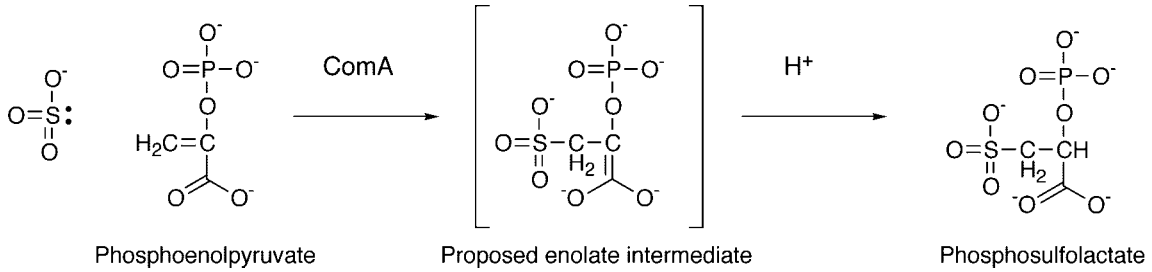

SCHEME 1. **The reaction catalyzed by ComA.**

than 15% sequence similarity, it is possible that more distantly related members may exist that have not yet been identified. One potentially unrecognized member of this superfamily is the *Methanococcus jannaschii* phosphosulfolactate synthase (ComA) or (2*R*)-*O*-phospho-3-sulfolactate sulfolyase (EC 4.4.1.19). Although this enzyme catalyzes an enolase-type reaction, the Mg^{2+} ion-dependent nucleophilic addition of sulfite to phosphoenolpyruvate (PEP),[1] it has no PEP hydratase (enolase) activity and has no significant sequence similarity to members of the enolase superfamily (11). Since many members of the enolase superfamily share only 15% or less sequence identity, there is the possibility that ComA is a distantly related enolase superfamily member. Alternatively, ComA may not be an enolase homologue at all, but has instead evolved an enolase-type mechanism independently as the result of convergent evolution.

Little is known about the mechanism of the reaction catalyzed by phosphosulfolactate synthase, which generates *R*-phosphosulfolactate by the stereospecific Michael addition of sulfite to phosphoenolpyruvate as the first step in coenzyme M biosynthesis (Scheme 1) (12). The lack of sequence similarity to any known enzyme makes inferences on the basis of sequence similarity difficult. Furthermore, with the exception of the SQD1/SqdB proteins in plants (13), which catalyze the addition of sulfite to UDP-glucose, no examples of sulfite chemistry in nature have been described.

Deuterium exchange experiments show that ComA catalyzes the exchange of the C2 proton of the product, *R*-phosphosulfolactate, which suggests that the reaction proceeds through an enolate intermediate (11). Such a mechanism would involve the nucleophilic addition of sulfite to an α,β-unsaturated carboxylic acid at the C3 position of phosphoenolpyruvate to generate an enolate anion intermediate. Like enolase, ComA requires the presence of Mg^{2+} for activity, which is presumably involved in the stabilization of the enolate intermediate. A general acid in the active site would protonate the *re* face of PEP to generate the product, *R*-phosphosulfolactate, in a stereospecific manner.

ComA from the hyperthermophile *M. jannaschii* consists of 251 amino acid residues with a molecular weight of 28,368. A sequence comparison shows that very few amino acid residues are strictly conserved among phosphosulfolactate synthase homologues except for a small number of aspartate and glutamate residues, some of which likely function as ligands for the metal ion (Asp^{40}, Glu^{103}, Glu^{133}, Glu^{168}, Glu^{171} and Glu^{205}). In addition, two lysine residues, Lys^{43} and Lys^{137}, are strictly conserved and may function as catalytic acids or be involved in sulfite binding. Some evidence exists that Lys^{137} may act as the catalytic acid that protonates the enolate intermediate. A K137N mutant was unable to catalyze the phosphosulfolactate synthase reaction or catalyze proton exchange at the C2 position, which would suggest that it plays a role in the protonation of the intermediate (11).

The lack of any structural information about phosphosulfolactate synthase has made it difficult to understand its reaction mechanism or to understand its relationship to other members of the enolase superfamily. While the evidence indicates that the phosphosulfolactate synthase reaction is mechanistically similar to that of enolase, it is unclear whether the two enzymes are homologous but highly divergent or are the result of convergent evolution in which an enolase-type mechanism evolved separately. To address these questions, we have determined the x-ray crystal structure of phosphosulfolactate synthase from *M. jannaschii* to 1.7 Å resolution.

MATERIALS AND METHODS

Protein Expression and Purification—M. jannaschii ComA protein was heterologously expressed in *Escherichia coli* as described previously (11). The protein was purified by ammonium sulfate precipitation followed by anion exchange chromatography over DEAE-Sepharose resin. The protein was concentrated to 15 mg/ml, dialyzed against 10 mM Tris-HCl, 1 mM $MgCl_2$, and drop-frozen in liquid nitrogen for storage at −80 °C.

Crystallization—Crystals of ComA were grown by the vapor diffusion hanging drop method from a well solution containing 1.6 M ammonium sulfate and 100 mM succinate at pH 4.4. Crystals grew to dimensions of ~150 μm after a few days. They belong to the cubic space group $P2_13$ with cell dimensions $a = b = c = 94$ Å. Crystals were transferred to a cryo-protecting solution similar to the original growth conditions but containing 15% ethylene glycol for ~30 s and were flash-frozen by placing them in a stream of nitrogen prior to diffraction experiments.

A platinum derivative for phasing purposes was prepared by soaking ComA crystals in a solution identical to the cryo-protecting solution that contained 5 mM K_2PtCl_4 for ~12 h. Crystals were flash-frozen by placing them in a stream of nitrogen prior to data collection.

Data Collection and Structure Determination—A native data set to 1.7-Å resolution was collected at beamline 14-BM of the Consortium for Advanced Radiation Sources at the Advanced Photon Source at Argonne National Laboratory (Argonne, IL) using a single 90° scan of 0.7° oscillations. The data were integrated and scaled with the programs denzo and scalepack (14). Data collection statistics are shown in Table I.

Initial phase information was obtained with technique of multiple wavelength anomalous dispersion utilizing data collected from the K_2PtCl_4 derivative crystals (15, 16). Diffraction data for K_2PtCl_4-soaked crystals were collected to beyond 2.0-Å at wavelengths corresponding to the peak and inflection point of the platinum absorbance edge as well as a remote wavelength. The data were integrated and scaled with the programs denzo and scalepack (14).

The structure was solved with the program SOLVE (17). Three platinum sites with full occupancy and one with partial occupancy were found. The phases from the three strong sites were used to calculate initial phases, which were improved by solvent flattening with the program RESOLVE. This strategy resulted in an interpretable map (18).

An initial model was built into the experimental density with the program TURBO FRODO (19). The model was improved with alternating rounds of model building and refinement with the program CNS (20). The final *R*-factor for the model was 17.3% and the final R_{free} was 19.2% for 5% of the data excluded from the refinement (20) (Table II). A Ramachandran plot as calculated with the program Procheck (21) indicates that 95% of non-glycine and non-proline residues fall in the most favorable region, 4.1% fall in the additionally allowed region, 0.5% fall in the generously allowed region, and one residue falls in a disallowed region. The electron density for this residue, Trp^{46}, however, was unambiguous. A representative section of electron density is shown in Fig. 1.

[1] The abbreviation used is: PEP, phosphoenolpyruvate.

TABLE I
Data collection statistics

	Peak	Edge	Remote	Native
Wavelength (Å)	1.0720	1.0722	1.0726	0.9792
Source	APS[a] 14-BM	APS 14-BM	APS 14-BM	APS 14-BM
Total reflections	293,934	337,185	354,582	446,003
Unique reflections	19,292	19,619	19,619	31,689
Resolution (Å)	2.00 (2.07–2.00)	2.00 (2.07–2.00)	2.00 (2.07–2.00)	1.7 (1.76–1.70)
R_{merge} (%)[b,c]	0.053 (0.067)	0.050 (0.066)	0.039 (0.048)	.028 (20.1)
Completeness (%)	98.4 (99.7)	99.9 (99.2)	99.9 (98.4)	88.5 (68.8)
Average I/σ	43.5 (36.7)	47.8 (36.7)	48.3 (42.3)	28.4 (4.7)

[a] APS, Advanced Photon Source at Argonne National Laboratory (Argonne, IL).
[b] $R_{merge} = (\Sigma|I_{hkl} - I|/(\Sigma I_{hkl})$, where the average intensity I is taken over all symmetry equivalent measurements, and I_{hkl} is the measured intensity for a given reflection.
[c] Statistics for the highest resolution bin.

TABLE II
Refinement statistics

Resolution	50–1.7 Å
No. of reflections working set	25,348
No. of reflections test set	1,294
No. of protein atoms[a]	1,980
No. of solvent atoms[b]	257
R-factor[c]	17.3
R_{free}	19.2
Root mean square deviation bond lengths	0.011 Å
Root mean square deviation bond angles	1.29°

[a] These include multiple conformations for Val^{34} and Ser^{222}.
[b] These include 242 water molecules and three sulfate ions.
[c] R-factor $= (\Sigma|F_o - F_c|/\Sigma F_o|) \times 100$, where F_o is the observed structure-factor amplitude, and F_c is the calculated structure-factor amplitude.

RESULTS AND DISCUSSION

Structure of the ComA Monomer—The crystallographic asymmetric unit contains one complete monomer of phosphosulfolactate synthase for which the electron density is continuous for the entire length of the protein from Met^1 to Val^{251}. The overall fold of the protein is an $(\alpha/\beta)_8$ barrel (TIM barrel) composed of eight parallel β-strands flanked by eight α-helices (Fig. 2). An N-terminal tail, formed from the first 13 residues, extends away from the barrel. While this tail is well ordered and clearly visible in the electron density, it is largely devoid of any well defined secondary structure elements. A shorter C-terminal tail, which contains a small 3:10 helical region, also extends away from the body of the barrel itself. In addition, several ordered secondary structural elements are inserted into the classic TIM barrel fold, including a short stretch of 3:10 helix after helix two and a long α-helix between β-strand three and helix three.

Structure of ComA Trimer—On the basis of a large buried surface area of ~1800 $Å^2$ between the ComA monomer and each of two other monomers related by a crystallographic 3-fold axis, the biological assembly of ComA was concluded to be a trimer. This observation corroborates the results of gel filtration experiments that suggested that the enzyme assembles as a trimer (11).

The three barrels in the trimer are oriented so that the C-terminal ends of each barrel faces roughly into the 3-fold axis (Fig. 3). Extensive interactions between the individual subunits in the trimer stabilize the oligomeric state. Side chains from residues located on the N- and C-terminal tails that extend away from the barrel form extensive hydrogen bonding and hydrophobic interactions with residues located on the two extra helices inserted into the $(\alpha/\beta)_8$ fold, located after β-strands two and three of the adjacent barrel in the trimer. Additional contacts are also made between these extra helical regions and helices seven and eight of the adjacent barrel.

ComA Active Site—The location of the enzyme active site was deduced from the location of a cluster of residues that are highly conserved in all known ComA homologues. This cluster of residues, which includes several glutamate and lysine residues, is found in a pocket formed by the interface of two subunits in the trimer. Thus, three active sites are created per trimer. Each active site is constructed primarily of residues from a single subunit but the other subunit at each interface also contributes a few key residues to the active site. The third subunit in the trimer does not contribute any residues to a given active site.

The side chains of several residues that are likely important for catalysis, including four conserved glutamate residues, are found clustered together in the active site. The first of these residues, Glu^{103}, is found at the end of the fourth β-strand and is strictly conserved across all known ComA homologues. The remaining three, Glu^{133}, Glu^{168}, and Glu^{205}, which are found at the ends of the fifth, sixth, and seventh β-strands, are highly conserved across almost all known ComA homologues. Given the location and arrangement of these conserved residues, it is likely that some or all of these are involved in the coordination of the metal ion required for catalysis. No metal ion was observed in the active site, however, so that the exact identity of the ligands for any Mg^{2+} ions in the active site could not be determined. Presumably the high concentrations of sulfate found in the crystal growth conditions chelated any free Mg^{2+} ions in solution and prevented them from binding in the enzyme active site.

Two ordered sulfate ions are present in the active site. The first (SA) is located toward the back of the active site pocket so that it is essentially buried from the solvent. This sulfate ion forms hydrogen bonds with the side chains of Lys^{43}, Lys^{137}, and Thr^{76} (Fig. 4). Additional contacts are made with the backbone amide hydrogen atoms of Thr^{76} and Trp^{46}. The second sulfate ion (SB), which is more solvent exposed, is coordinated by the side chain of Arg^{170}, the main chain amide hydrogen atom of Glu^{171}, and the side chain or $Arg^{244'}$ from the second subunit in the active site. The side chain of $Arg^{244'}$, which is located on the C-terminal tail region, participates in a stacking interaction with the indole side chain of Trp^{46}. The nitrogen of the Trp^{46} side chain, in turn, forms a hydrogen bond with the oxygen atom of the side chain of $Thr^{238'}$ from the second subunit in the active site. As mentioned above, Trp^{46} was observed to be in a strained conformation, which suggests that the position of the indole ring and the interactions it makes with residues from the second monomer might be critical for active site assembly at the interface and the orientation of the $Arg^{244'}$ side chain.

Model for Binding of PEP—Numerous attempts were made to obtain crystals of ComA with a substrate, product, or substrate analogue in the active site either by soaking ComA crystals or co-crystallizing ComA with these various compounds. Unfortunately, diffraction quality crystals were not obtained. Given the extensive contacts made between the two

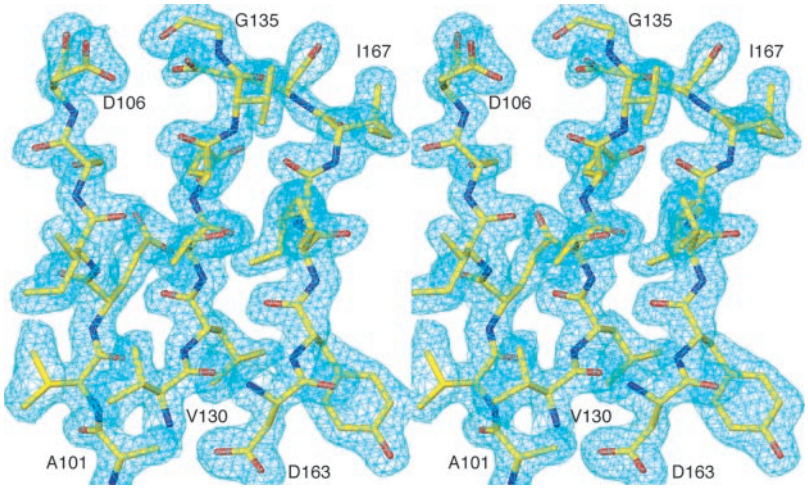

FIG. 1. **Stereo view of representative electron density.** The map was calculated with coefficients of the form $2F_o - F_c$ map and was contoured at 1 σ. Electron density is shown for β-strands four, five, and six. The figure was prepared with the program Ribbons (23).

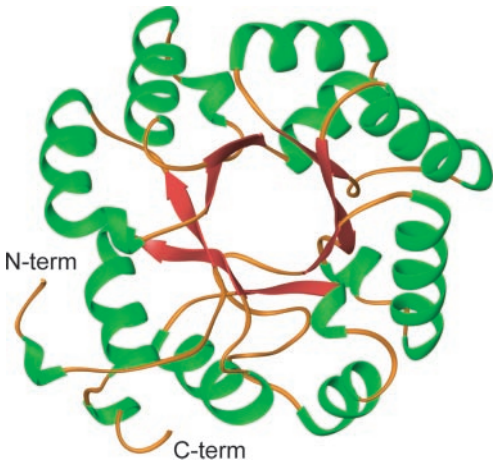

FIG. 2. **Ribbon representation of the ComA monomer found in the crystallographic asymmetric unit.** The figure was prepared with the program Ribbons (23).

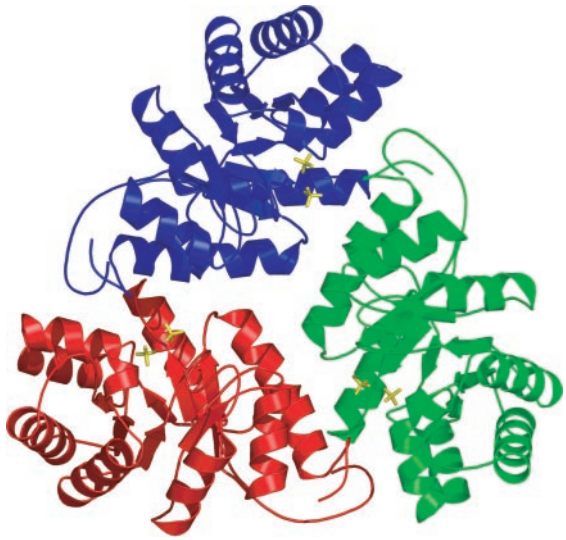

FIG. 3. **Ribbon representation of the ComA trimer.** The view is looking straight down the crystallographic 3-fold axis. The locations of the three active sites are indicated by the locations of the two ordered phosphate ions shown in *ball-and-stick* form. Each active site lies at a subunit interface so that two subunits contribute to each active site. The figure was prepared using the program Ribbons (23).

sulfate ions and conserved residues in the active site, however, it is likely that these two sulfate ions are bound in positions analogous to those of the phosphate group of PEP and sulfite.

While it is difficult to know for certain which sulfate ion is analogous to the phosphoryl group of PEP and which is analogous to sulfite, only the deeper buried sulfate ion has sufficient space around it to accommodate phosphoenolpyruvate. Accordingly, PEP can be modeled into the active site by overlaying the phosphate group on top of the sulfate ion that is more deeply buried in the active site (SA). The most plausible orientation for the molecule places the phosphate group of PEP near the side chains of Glu^{103} and Glu^{133}. In this orientation, a Mg^{2+} ion, bound by the side chains of Glu^{103} and Glu^{133}, could bind to an oxygen atom on the phosphate group of PEP and one of the oxygen atoms of the carboxyl group of PEP (Fig. 5). This Mg^{2+} ion would function to assist in the binding of PEP by offsetting the negatively charged phosphate group. The carboxyl group of PEP would lie near the side chains of Glu^{168} and Glu^{205}. These two side chains might function to bind a second Mg^{2+} ion that could serve to coordinate the two oxygen atoms of the carboxyl group of PEP. The use of two Mg^{2+} ions to bind PEP is consistent with biochemical evidence that suggests several molar equivalents of Mg^{2+} bind to PEP in the active site (11). Such an arrangement would be similar to that seen in the active site of enolase (8, 22).

Role of Active Site Residues—The likely mechanism for the ComA catalyzed reaction involves the Michael addition of sulfite to carbon C3 of PEP to generate an anion intermediate. This intermediate, the most stable form of which would be the enol form, would then be protonated in a second step by a general acid in the active site to produce the product, phosphosulfolactate. The ability of ComA to catalyze the exchange of the proton on carbon C2 of only the *R* enantiomer of the ComA reaction product, phosphosulfolactate, supports this mechanism and suggests the protonation must occur from the *re* face, which is consistent for the observed stereochemistry of the enzyme-catalyzed reaction as determined by NMR spectroscopy (11). Consequently, sulfite would add to the *si* face of PEP.

The position of the more solvent exposed sulfate molecule in the active site (SB), which is likely analogous to the position of sulfite, is within 2 Å of the proposed location of carbon C3 of PEP and would place the sulfite ion in an ideal position for addition to PEP. The side chains of Arg^{170} and $Arg^{244\prime}$, which form hydrogen bonds with three of the four oxygen atoms on the sulfate ion, likely function to orient and position the reactive sulfite ion so that the lone pair of electrons on the sulfur atom of sulfite are positioned for addition to carbon C3 of PEP. The stacking interactions between the side chain of Trp^{46} and the side chain of $Arg^{244\prime}$, which is donated by the second subunit in the active site interface, may be important for orienting the arginine side chain correctly and may also be important for bringing

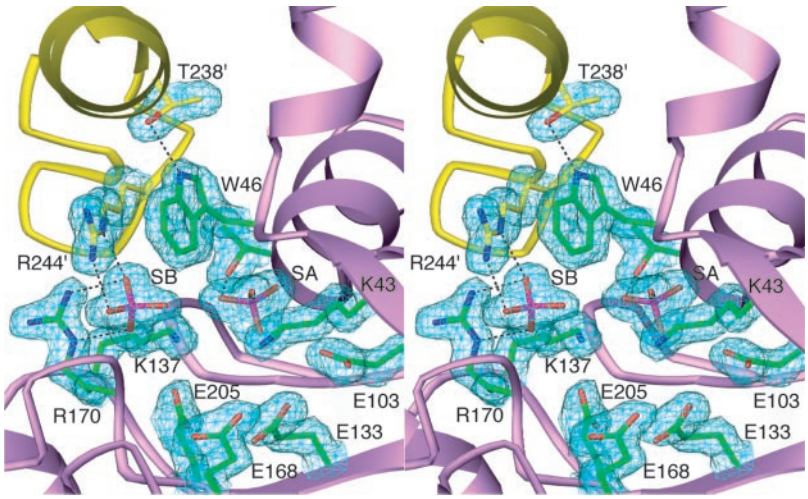

FIG. 4. **Stereo view of the ComA active site and sample electron density.** The subunit that makes up most of the active site is shown in *lavender*. Side chains from residues from this subunit are shown in *green*. The other subunit is shown in *yellow*. The two ordered sulfate ions each make several contacts with conserved active site residues. The more solvent exposed sulfate ion (SB) forms contacts with residues from both subunits at the interface, while the buried sulfate ion (SA) makes contacts with only the major subunit in the active site interface. The positions of several conserved glutamate residues, which are believed to serve as ligands for the Mg^{2+} ions, are shown. Electron density for selected active site residues is shown from a $2F_o - F_c$ map contoured at 1 σ. The figure was prepared using the program Ribbons (23).

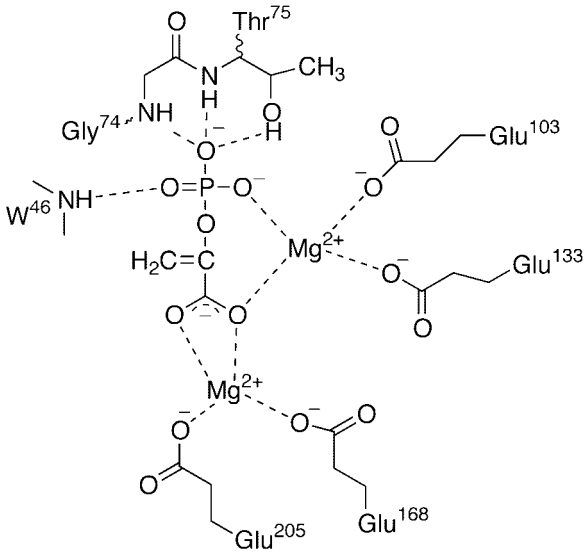

FIG. 5. **Schematic showing a possible binding mode for PEP.** The negative charges of the phosphate group and the carboxylate group of PEP are offset by two Mg^{2+} ions. Several conserved aspartate residues in the active site are proposed to act as ligands for the two Mg^{2+} ions.

together the individual subunits that form the active site.

The role of the general acid likely falls on one of two conserved lysine residues, Lys^{43} or Lys^{137}, located in the active site. The ϵ-amino groups of these two lysine side chains are both near the proposed binding site for PEP. A K137N mutant was unable to catalyze either the synthase reaction or the proton exchange reaction, which suggests that Lys^{137} acts as the general acid (11). Further biochemical and structural analysis will be required to determine the exact roles of these residues in the ComA reaction.

Comparison to Enolases—Because of the lack of significant sequence identity to any known enzyme, little can be inferred about the mechanism and function of ComA from its sequence alone. In addition, there are few examples of enzymes the bind sulfite and little is understood about biological sulfite chemistry. Thus, sequence analysis or comparison to related enzymes does not provide much insight into sulfite catalysis. The ComA reaction, like those of enolase superfamily members, appears to proceed via an enolate intermediate that is generated through the abstraction of a proton α to a carboxylate group. Like enolases, ComA requires one or more Mg^{2+} ions for catalysis to bind and stabilize the negatively charged enolate intermediate. Also like enolases, the ComA active site contains a host of conserved aspartate and glutamate side chains that function as ligands for the Mg^{2+} ions.

Several key differences from enolases exist, however. The most prominent is that ComA consists of a single domain in the form of a standard $(\alpha/\beta)_8$ barrel fold instead of the two-domain fold that is shared by the enolase superfamily. In enolases, the N-terminal $\alpha+\beta$ domain is thought to "cap" the end of the C-terminal barrel domain and confer substrate specificity on the reaction. While residues exist in the active site of ComA that could serve a similar function, they are located on the adjacent monomer that helps to form the ComA active site. In effect, the trimeric assembly of ComA may be seen as performing a similar function to the multidomain structure of enolases. The use of quaternary interactions to create an active site cap allows for a shorter polypeptide chain than observed for members of the enolase superfamily.

A second, more critical difference between ComA and enolases is that while both enzymes employ a group of conserved aspartate and glutamate residues to act as ligands to the Mg^{2+} ions, the identity of these residues is not the same in ComA as in enolases. The residues that function as ligands for the metal ions in enolases are an aspartate residue at the C-terminal end of the third β-strand, a glutamate residue at the end of the fourth β-strand, and either an aspartate or a glutamate residue at the end of the fifth β-strand. These residues are not conserved in ComA. Instead the residues that likely coordinate the Mg^{2+} ions are three or possibly four glutamate residues found at the C-terminal ends of the fourth, fifth, sixth, and possibly seventh β-strands. These large differences in the overall structure and the active sites of ComA and enolase superfamily members, combined with the lack of any significant shared sequence identity between them, suggest that ComA and enolase superfamily members did not evolve from a common ancestral enzyme, even though they catalyze similar reactions with similar mechanisms.

Conclusions—The reaction mechanism of phosphosulfolactate synthase encoded by the ComA gene of *M. jannaschii* likely involves the formation of an enolate anion in a manner similar to that observed in members of the enolase superfamily. Like enolases, the active site of ComA contains several conserved acidic amino acid side chains that could act as ligands for one or more Mg^{2+} ions that are used by the enzyme to stabilize the negatively charged enolate intermediate. Nevertheless, the lack of any sequence identity, structural similarity, or conservation in active site residues to any known enolase suggests that while ComA appears to be mechanistically similar to enolases, it is not a member of the enolase superfamily. Instead, ComA appears to have evolved to use a mechanism similar to

that of enolases by convergent evolution. Further biochemical and structural studies will be necessary to understand better the mechanistic relationship between ComA and the enolase superfamily.

Acknowledgment—We thank John Gerlt (University of Illinois) for helpful discussions.

REFERENCES

1. Gerlt, J. A., and Babbitt, P. C. (2001) *Annu. Rev. Biochem.* **70,** 209–246
2. Schmidt, D. M., Hubbard, B. K., and Gerlt, J. A. (2001) *Biochemistry* **40,** 15707–15715
3. Gerlt, J. A., and Raushel, F. M. (2003) *Curr. Opin. Chem. Biol.* **7,** 252–264
4. Babbitt, P. C., Hasson, M. S., Wedekind, J. E., Palmer, D. R., Barrett, W. C., Reed, G. H., Rayment, I., Ringe, D., Kenyon, G. L., and Gerlt, J. A. (1996) *Biochemistry* **35,** 16489–16501
5. Landro, J. A., Gerlt, J. A., Kozarich, J. W., Koo, C. W., Shah, V. J., Kenyon, G. L., Neidhart, D. J., Fujita, S., and Petsko, G. A. (1994) *Biochemistry* **33,** 635–643
6. Hasson, M. S., Schlichting, I., Moulai, J., Taylor, K., Barrett, W., Kenyon, G. L., Babbitt, P. C., Gerlt, J. A., Petsko, G. A., and Ringe, D. (1998) *Proc. Natl. Acad. Sci. U. S. A.* **95,** 10396–10401
7. Helin, S., Kahn, P. C., Guha, B. L., Mallows, D. G., and Goldman, A. (1995) *J. Mol. Biol.* **254,** 918–941
8. Larsen, T. M., Wedekind, J. E., Rayment, I., and Reed, G. H. (1996) *Biochemistry* **35,** 4349–4358
9. Thompson, T. B., Garrett, J. B., Taylor, E. A., Meganathan, R., Gerlt, J. A., and Rayment, I. (2000) *Biochemistry* **39,** 10662–10676
10. Babbitt, P. C., Mrachko, G. T., Hasson, M. S., Huisman, G. W., Kolter, R., Ringe, D., Petsko, G. A., Kenyon, G. L., and Gerlt, J. A. (1995) *Science* **267,** 1159–1161
11. Graham, D. E., Xu, H., and White, R. H. (2002) *J. Biol. Chem.* **277,** 13421–13429
12. Graham, D. E., and White, R. H. (2002) *Nat. Prod. Rep.* **19,** 133–147
13. Sanda, S., Leustek, T., Theisen, M. J., Garavito, R. M., and Benning, C. (2001) *J. Biol. Chem.* **276,** 3941–3946
14. Otwinowski, Z., and Minor, W. (1997) *Methods Enzymol.* **276,** 307–326
15. Hendrickson, W. A. (1991) *Science* **254,** 51–58
16. Ramakrishnan, V., and Biou, V. (1997) *Methods Enzymol.* **276,** 538–557
17. Terwilliger, T. C., and Berendzen, J. (1999) *Acta Crystallogr. D. Biol. Crystallogr.* **55,** 849–861
18. Terwilliger, T. C. (2000) *Acta Crystallogr. D. Biol. Crystallogr.* **56,** 965–972
19. Roussel, A., and Cambillau, C. (1991) in *Silicon Graphics Geometry Partners Directory*, Vol. 86, Silicon Graphics, Mountain View, CA
20. Brunger, A. T., Adams, P. D., Clore, G. M., DeLano, W. L., Gros, P., Grosse-Kunstleve, R. W., Jiang, J. S., Kuszewski, J., Nilges, M., Pannu, N. S., Read, R. J., Rice, L. M., Simonson, T., and Warren, G. L. (1998) *Acta Crystallogr. Sect. D Biol. Crystallogr.* **54,** 905–921
21. Laskowski, R. A., MacArthur, M. W., Moss, D. S., and Thornton, J. M. (1993) *J. Appl. Crystallogr.* **26,** 283–291
22. Faller, L. D., Baroudy, B. M., Johnson, A. M., and Ewall, R. X. (1977) *Biochemistry* **16,** 3864–3869
23. Carson, M. (1997) *Macromolecular Crystallography, Part B* **277,** 493–505